Mater. Res. Soc. Symp. Proc. Vol. 901E © 2006 Materials Research Society 0901-Ra15-01.1

How to realize ultimate spatial and temporal resolutions by laser-combined scanning tunneling microscopy?

Hidemi Shigekawa*, Osamu Takeuchi, Masahiro Aoyama, Yasuhiko Terada,
Hiroyuki Kondo and Haruhiro Oigawa
Institute of Applied Physics, CREST, 21st COE, University of Tsukuba,
Tsukuba 305-8573 Japan
* http://dora.ims.tsukuba.ac.jp/

Abstract

By combining scanning tunneling microscopy (STM) and the optical pump-probe technique using a femtosecond pulse laser, we have developed a new microscopy, shaken pulse-pair-excited STM (SPPX-STM), that enables us to observe the dynamics of electronic structures with the ultimate spatial and temporal resolutions.

1. Introduction

At present, smaller and faster are the keywords in nanoscale science and technology. Actually, important and interesting phenomena occurring in various systems, such as functional materials, electronic devices, signal transfer in biosystems, and chemical reactions, are observed at several tens of nanometer to the single-molecule level in space and in the several tens of picosecond to subpicosecond range in time. However, it is extremely difficult to realize spatial and temporal resolutions simultaneously on this scale. Therefore, to determine the possibilities of realizing such resolutions, it is necessary to develop a new method. That is what we have been challenging to do, namely, the development of a new microscopy, the laser-combined scanning tunneling microscopy (STM) [1-6].

STM has an excellent spatial resolution on the subangstrom scale, but, its temporal resolution is limited to ~100kHz. In contrast, the ultrashort pulse laser technique enables the observation of electronic dynamics in the femtosecond range, but its spatial resolution is generally limited by wavelength. Therefore, it is desired to combine these two techniques to realize the ultimate spatial and temporal resolutions simultaneously.

2. Electronic structures on nanoscale.

In the world of nanofactories, as illustrated in Fig. 1, elemental blocks with various characteristics are integrated and organized on a designed stage to produce desired or new functions in a system on the macroscopic scale. However, to realize such a goal, the characterization and control of the structures of each

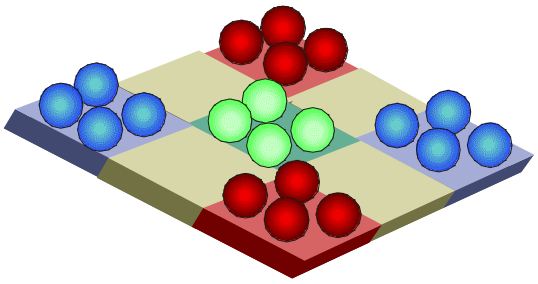

Figure 1. Schematic model of nanoscale system.

element are essential. Let us see two examples.

Figures 2(a) and 2(b) show an STM image of a Si nanoparticle of ~3nm diameter on a graphite surface and the cross sections of the same region obtained at different bias voltages, respectively. Inhomogeneous structures are observed in the cross sections. Since STM provides information on the electronic structures at the observed bias voltage, the results indicate that there are complex electronic structures even at the single-molecule level. How can complex local dynamics work to produce a systematic function on the macroscopic scale?

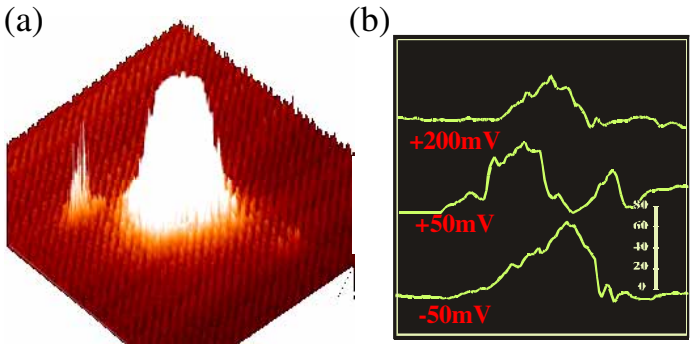

Figure 2. STM image of Si nanoparticle (a) and cross section of the same region obtained at different bias voltages (b).

Figure 3 shows bias-voltage-dependent surface photovoltage (SPV) images of a Ag/Si(011) surface nanostructure. The Ag islands formed on the Si(001) surface are marked by green lines in Fig. 3(a). Figures 3(b) to 3(d) show the mappings of SPV measured at different bias voltages by light-modulated scanning tunneling spectroscopy (LM-STS) [7,8]. The differences are variations in the depth of the depletion layer with applied bias voltage due to tip-induced band bending [9]. Since SPV is related to the local carrier dynamics induced by photoillumination, three-dimensional electronic structures can be observed by this technique. What is desired next is to probe the dynamics of fast change of electronic structures on the nanoscale.

Can we obtain information on the above-mentioned nanoscale dynamics by STM?

3. Observation of dynamics of electronic structures by STM

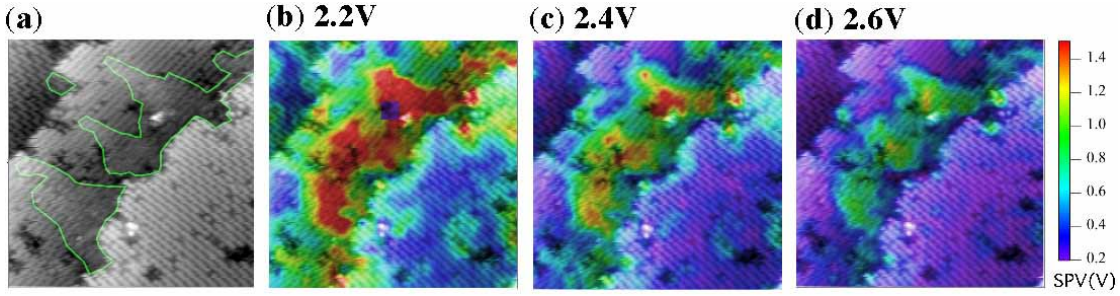

Figure 3. Bias-voltage-dependent surface photovoltage (SPV) images obtained for Ag/Si(011) surface nanostructures (30nm x 30nm).

In STM, we place a sharp tip close to the target material. Information on the region underneath the STM tip is probed by tunneling current. What is imaged by STM is in general a structure under an equilibrium condition. However, when some perturbations in conditions, such as temperature, electric field and photoillumination, are added from outside, we can analyze the dynamics of the system by observing responses to the change in the conditions.

Figure 4(a) shows the structure of the azobenzene molecule. This molecule changes its conformation between trans and cis forms under visible (Vis, 440nm) and ultraviolet (UV, 360nm) lights. Therefore, when functional molecules are modified using this molecule, new functions associated with switching mechanisms can be added to the original functions such as molecular recognition, sensing, and memory, as shown in Fig. 4(b). Thus, it is very important to analyze the structural change of the azo-molecule ([4-(phenyldiazenyl)phenyl]-*N*-(2-sulfanylethl)carboxyamide) at the single-molecule level.

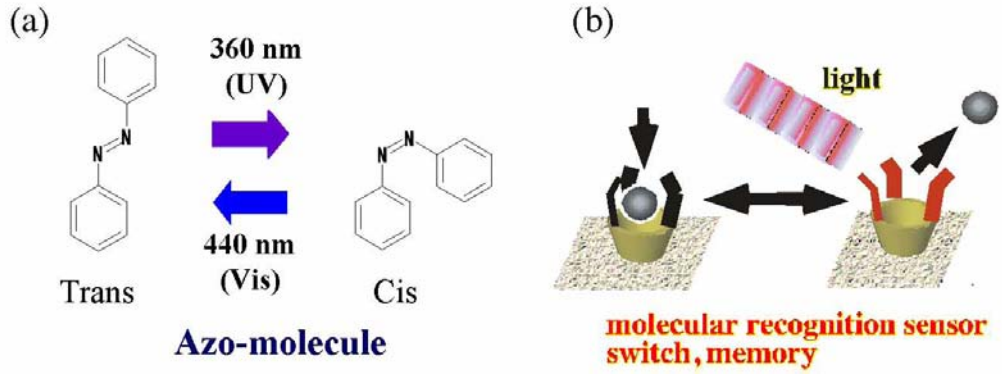

Figure 4. (a) Schematic of photoisomerization of azobenzene molecule. (b) Schematic of functional control using an azobenzene molecule.

Figure 5(a) shows a schematic of the STM setup [10]. The STM tip is placed just above an isolated

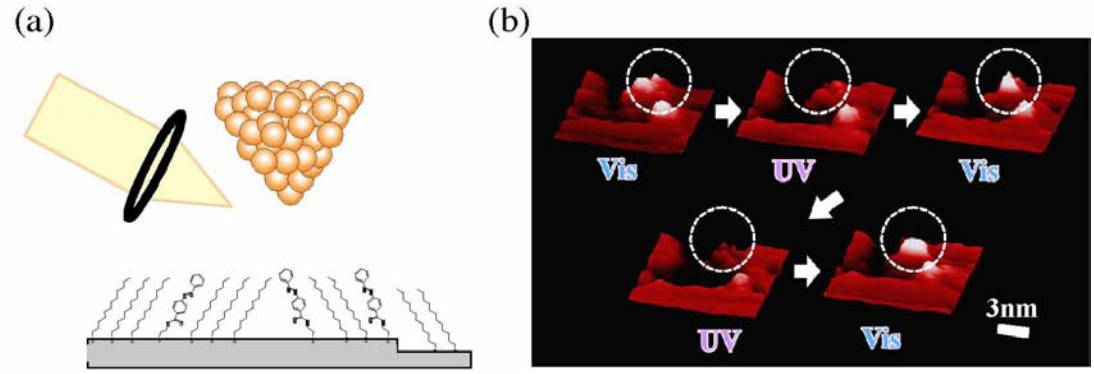

Figure 5. (a) Schematic of STM measurement setup. (b) Photoisomerization of azobenzene molecule directly observed by STM. Vis and Uv indicate visible and ultraviolet lights, respectively.

azo-molecule embedded in a *n*-dodecanethiol (C_{12}) self-assembled monolayer (SAM) film formed on a Au(111) substrate. Samples were prepared by dipping gold-coated mica substrates into a solution with the target azo-molecule, and dodecanthiol molecules that were used as spacers to isolate azo-molecules. A photo-induced structural change was observed by STM under photoillumination with the wavelength varied between Vis and UV wavelengths alternately. Since an azo-molecule has a longer conformation in the trans form, it is supposed to be brighter under Vis light.

Figure 5(b) shows the result of direct observation of the conformational change. The azo-molecule reversibly changes its image from bright to dark under Vis and UV lights, respectively, as expected. This change can be observed by STM at the single-molecule level. When we change temperature, we can observe temperature-dependent phase transition of materials at atomic resolution [9, 11-16]. However, it requires a long time to image such structural changes, for example, one minute per each image.

Without imaging, we can more rapidly observe structural changes. Figure 6(a) shows a schematic of such measurement. An STM tip is held just above a target, for example, a Si dimer on a Si(011) surface which rapidly flip-flops between two conformations even at 80K [17]. Since tunneling current depends on the distance between the STM tip and the target material, structural changes can be determined from the corresponding change in tunneling current. Figure 6(b) shows the time dependence of tunneling current measured by STM with the tip held just above the same Si dimer. Tunneling current changes between two well-defined states, as expected. In this way, we can observe the dynamics of faster structural changes.

This method can be used to analyze the change in the dynamics of a single molecule [10]. However, as mentioned in the introduction, the maximum temporal resolution of STM is limited to ~100kHz.

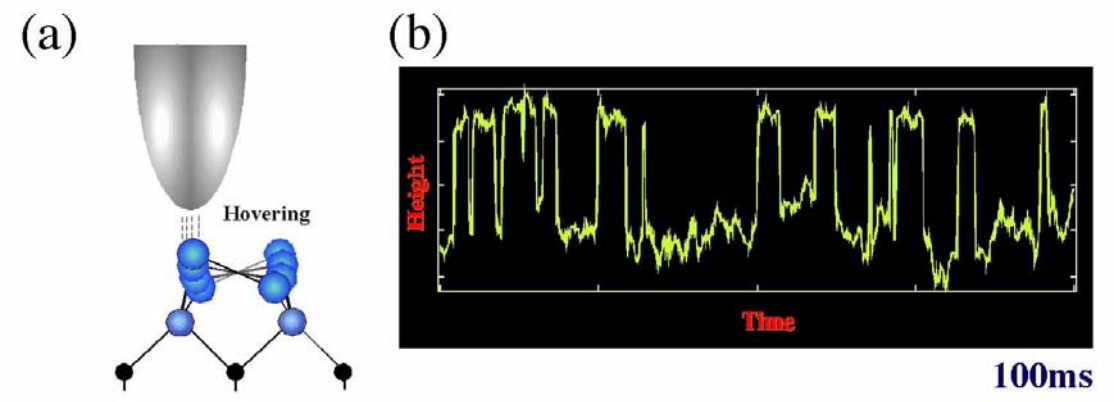

Fig. 6. Schematic of STM setup for observing flip-flop motion of Si dimer (a) and its result (b). Tunneling current changes between two well-defined states.

4. Optical pump-probe technique

Let us see here briefly how fast another method, namely, the optical pump-probe technique, is [5, 18]. When ultrashort laser pulses are produced at 80MHz, the original pulse train has a ~10ns time distance between two subsequent pulses, as shown in Fig. 7(b). Each pulse is divided into two pulses with a certain delay time (Fig. 7(a)) to form a train of pulse pairs, as shown in Fig. 7(c). We can control delay time by changing the optical length of the delay time system shown in Fig. 7(a).

First pulses are used as a pump to excite the sample surface and second pulses are used as a probe to observe the relaxation of the excited state induced by the pump pulse, as shown in Fig. 8(a). Since the

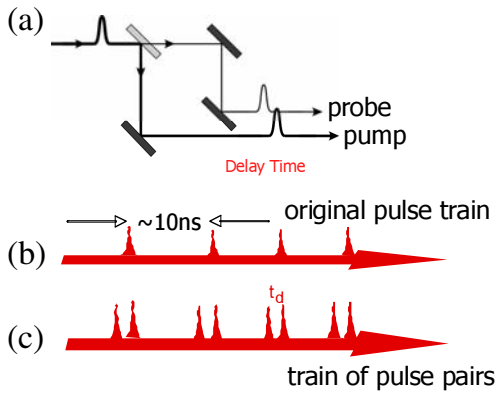

Figure 7. (a) Schematic of optical delay time system. (b) Original laser pulse train oscillating at 80MHz. (c) Train of laser pulse pairs.

reflectivity of the second pulses depends on the surface conditions, if the reflectivity of such pulses is measured as a function of delay time, we can obtain information on the relaxation of the excited state through the change in reflectivity (Fig. 8(b)). In this case, time resolution is limited only by the pulse width, namely, in the ~1fs range.

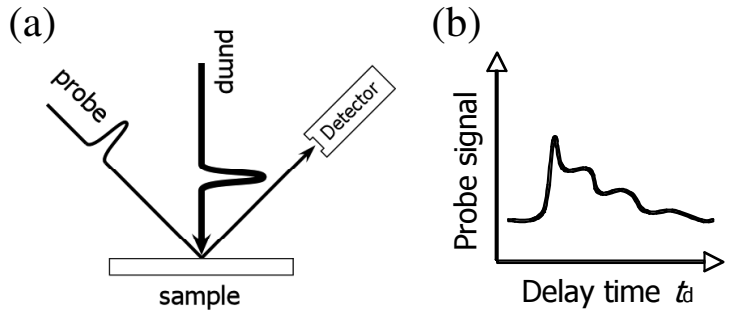

Figure 8. Schematics of optical pump-probe measurement system (a) and obtained signal (b).

For comparison, a spectrum of GaAs sample obtained by the optical pump-probe technique is shown in Fig. 9. The reflectivity of the second pulses is plotted as a function of delay time, which shows the relaxation of the excited state in the picosecond range. The signal consists of two components' lifetimes which are ~0.8ps and ~10 ps. These dynamics are attributed to the intra- and inter-band transitions of photocarriers [18].

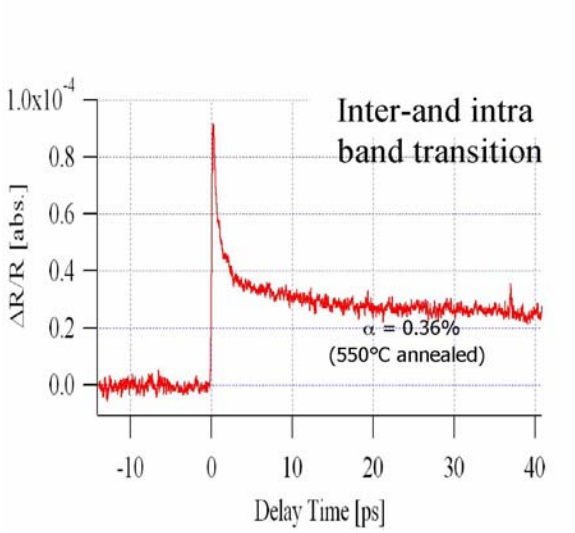

Figure 9. Result obtained by optical-pump-probe technique for GaN_xAs_{1-x} (x=0.36%) sample.

5. Difficulties in combining STM with optical pump-probe technique

Now, one may want to combine the two techniques to achieve the ultimate resolutions in space and time simultaneously. However, there are many difficulties we have to overcome [5]. Let us see two examples.

5-1. Temporal resolution of STM

As has been mentioned, the temporal resolution of STM is limited to ~100kHz, worse than 10 μ s. Therefore, although an ultrashort pulse laser has now provided a temporal resolution of ~1fs, we still cannot observe the dynamics of a fast change, for example, in the picosecond range, by STM (Fig. 10). Since the development of STM, many researchers have pursued this goal [5, 19-23], but have not yet succeeded completely. Thus probing the dynamics of a fast change based on tunneling current is a critical point.

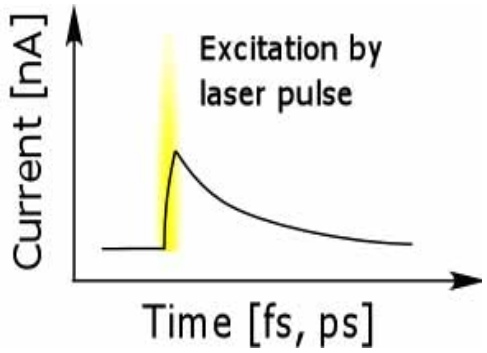

Figure 10. Change in tunneling current excited by ultrashort laser pulse.

5-2. Thermal expansion of STM tip

Tunneling current depends exponentially on tip-sample distance, namely, when the distance changes by 0.1nm, tunneling current changes one order. Therefore, it is a critical problem that we have to solve [1, 2, 5].

Figure 11 shows the change in tunneling current as a function of time, representing the stability of

tunneling current. A tungsten tip and a Au(111) surface were used for the measurement. As Fig. 11(a) shows, the signal obtained without photoillumination is very stable; however, when the tunnel gap is photoilluminated with chopped light, tunneling current is modulated at the same frequency due to the thermal expansion and shrinking of the STM tip and the sample surface, as shown in Fig. 11(b).

As will be discussed in the next section, we need to modulate the excitation to use a lock-in technique for measuring the weak target signal induced by ultrashort laser pulses. Since the change in tunneling current due to thermal expansion is large, the elimination of this thermal expansion effect is another critical problem that we have to overcome to realize the combination of STM with the ultrashort pulse laser technique.

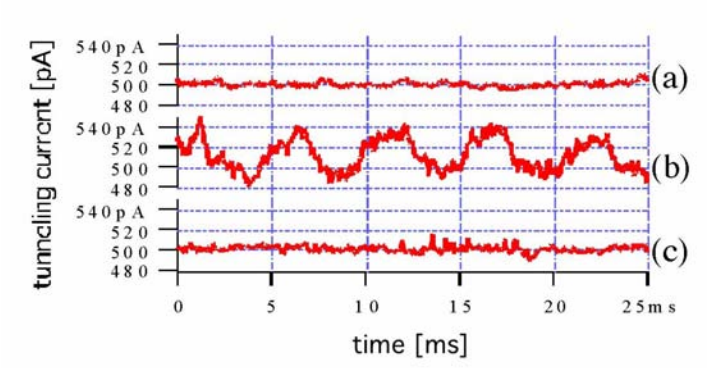

Figure 11. Tunneling current with time obtained (a) without photoillumination, (b) under chopped light, (c) by our method, shaken pulse-pair-excited STM.

6. How to combine STM with optical pump-probe technique?

6-1. How to observe fast dynamics by STM?

Since the development of STM, many researchers have expended effort to observe fast dynamics by STM. The ultimate goal is to analyze the electronic and structural dynamics of materials on the femtosecond scale at atomic resolution.

There have been two major concepts proposed for achieving this goal [19-25]. One is to introduce an ultrafast photoconductive gate into the current detection line of STM. This type of microscopy is called "photoconductively gated STM". Two laser beams consisting of a train of laser pulses are used to excite a sample and switch the photoconductive gate. The photoconductive gate enables the sampling of instantaneous tunneling current induced on the sample by the excitation laser pulses. When the current is recorded as a function of the delay time between excitation and gating, transient tunneling current is presumed to be reproduced on a real-time scale. However, the detected signal is primarily due not to tunneling current, but to the displacement current generated by the coupling of two stray capacitances, one at the tunneling junction and the other at the photoconductive gate.

In another approach, a tunneling junction is excited by a sequence of laser pulses and induced tunneling

current is measured as a function of interpulse spacing.

As pioneering work, the carrier relaxation time at the Si(111)-7x7 surface was determined with an approximately 10 ns time resolution and a 1 μm spatial resolution. The sample surface just under the STM tip was irradiated with a train of laser pulses. Because surface potential is modulated by the irradiation due to the surface photovoltage effect, displacement current can be probed using the STM tip when the irradiation is switched from on to off, and vice versa. As displacement current depends on the change in band bending during the interpulse period of the laser pulses, the signal as a function of the repetition time of the laser pulses provides information on the band relaxation mechanism. This technique is applicable, but the spatial resolution is limited to ~1μm, since the signal is displacement current. Moreover, since the repetition rate of laser pulses is changed by thinning out laser pulses from the original pulse train, time resolution is limited by the repetition rate of the original pulse train, ~100MHz (10ns).

To obtain a time resolution higher than the repetition rate, a new method, called "pulse-pair-excited STM" was proposed [2, 5, 6]. Tunneling current measurement by STM ensures atomic spatial resolution.

6-2. Pulse-pair-excited STM

For the conventional optical pump-probe technique, as shown in Fig. 8(a), the electronic structures of a target material are excited by the pump laser pulses and then relax with time. The reflectivity of the second laser pulses is measured as a function of delay time. Thus, the change in the reflectivity with delay time is analyzed as a signal associated with the relaxation of the excited state (Fig. 8(b)) [5, 18].

For a laser-combined STM, the sample surface just under the STM tip is similarly photoilluminated with the paired pulses. Average tunneling current is measured as a function of delay time instead of the reflectivity of the second pulses. Let us determine the probe for a pulse-pair-excited STM. Figure 12 shows the relationship between the tunneling current induced a pair of laser pulses and the delay time of the two pulses. When the delay time is large, change in the tunneling current induced by the two laser pulses contributes to the average tunneling current independently, and their amounts are the same. For a delay time shorter than the

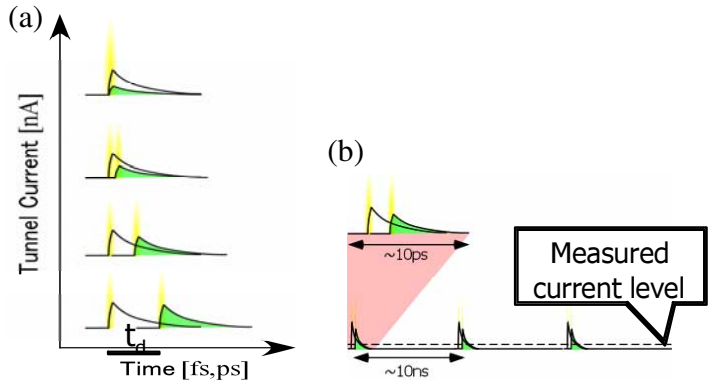

Figure 12. Relationship between tunneling current induced by paired laser pulses and delay time of the two pulses.

relaxation time of the excited state induced by the first pulse, and for the nonlinear interference between excitations by the two pulses, the tunneling current induced by the second pulses depends on delay time. In such a case, average current also changes as a function of the delay time. Thus, the dynamics of the electronic structure of a target material can be probed on the basis of tunneling current, at the pulse width resolution, namely, in the femtosecond range.

6-3. How to treat thermal expansion?

Since the signal is very weak, we need to use a lock-in detection measurement. In such a case, excitation is modulated at a certain frequency and the corresponding change in tunneling current is measured as a signal. However, as mentioned in section 5-2, intensity modulation strongly influences the stability of tunneling current. What we did is to modulate delay time instead of intensity, in which modulation frequency was chosen independently of that of any noises. Figure 11(c) shows the stability of the tunneling current measured by this method under photoillumination. To evaluate the thermal expansion effect caused by photoillumination, we used a Au surface as a sample in which little photoinduced signal is expected to occur. Actually, no thermal expansion effect shown in Fig. 11(b) was observed in this case, indicating the possibility for measuring the weak target signal with our method.

6-4. Shaken pulse-pair-excited STM (SPPX-STM)

Figure 13 shows a schematic of the femtosecond time-resolved STM that we developed. Each laser pulse is divided into two pulses to form a train of pair pulses. The sample just under the STM tip is photoilluminated and average tunneling current is measured as a function of delay time. Since the lock-in method is used to measure a weak signal with the modulation of delay time, the first signal obtained is differentiated tunneling current, which is a function of delay time. Therefore, after the numerical integration of the signal, we can obtain a spectrum that we can compare with that obtained by the conventional optical pump-probe technique.

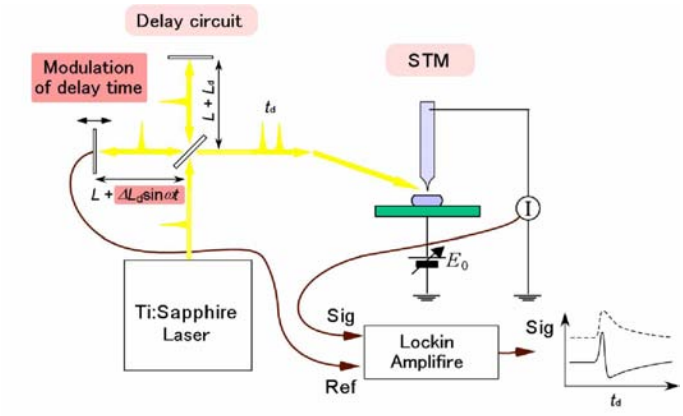

Figure 13. Schematic of shaken pulse-pair-excited STM system.

7. Results of SPPX-STM

Figure 14 shows the result obtained by SPPX-STM for a GaAs sample. As is explained in section 6-3,

differentiated spectrum is obtained first as shown in Fig. 14 by black lines for in-phase (upper) and out-of-phase (lower) signals. By the numerical integration of the in-phase signal, tunneling current deviation can be obtained as drwan in the red graph, which can be compared with that in Fig. 9.

As shown in Fig. 14, tunneling current changes in the picosecond range; however, the shape of the

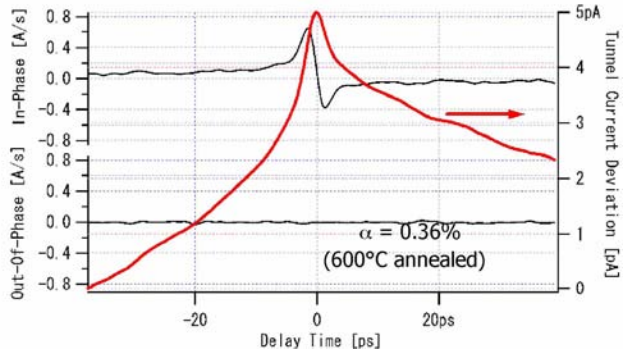

Figure 14. Result obtained by SPPX for GaN_xAs_{1-x} (x=0.36%) sample.

spectrum may differ from that obtained by the optical pump-probe technique. Because the probe is tunneling current in this case, the signal appears even in the negative-delay-time region. The asymmetry of the signals between the positive- and negative-delay-time regions is due to the difference in intensity between the pump and probe pulses. The signal consists of two components' lifetimes are ~0.5ps and ~50ps, which are in good agreement with these obtained by the optical pump probe technique. To confirm that what we observed is tunneling current, we measured the change in signal intensity as a function of total tunneling current by changing the distance between the tip and the sample. As shown in Fig. 15, there is a clear linear relationship between these parameters, indicating that the signal is tunneling current and not other signals, i.e., those caused by photoemission observed in previous work [2,5,19-25].

Since tunneling current is measured as probe in this method, fast dynamics can be observed principally at STM resolution.

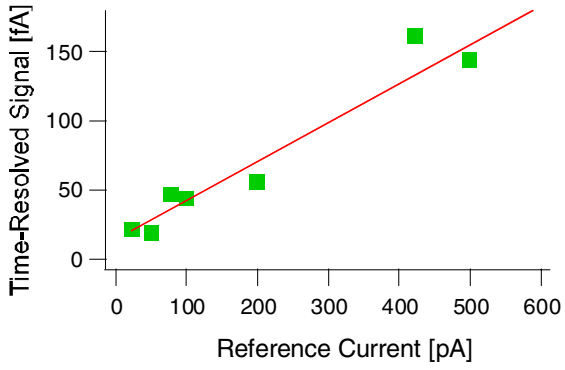

Figure 15. Relationship between time-resolved signal intensity and average tunneling current, measured while varying tip-sample distance.

8. Conclusion

We have been developing a new femtosecond time-resolved STM, shaken pulse-pair-excited STM (SPPX-STM), and have obtained partial results. We hope that our new technique will contribute to advance future research in nanoscale science and technology, in terms of the ultimate temporal and spatial resolutions.

This work was supported in part by a Grant-in-Aid for Scientific research from the Ministry of Education, Culture, Sports, Science, and Technology of Japan. We thank Ms. Rie Yamashita, in our group at University of Tsukuba, for her help in preparing this paper.

References

1. O.Takeuchi, R.Morita, M.Yamashita and H. Shigekawa, *Jpn. J. Appl. Phys.* 41, 7B, 4994-4997 (2002).
2. O. Takeuchi, M. Aoyama, R. Oshima, Y. Okada, H. Oigawa, N. Sano, R.Morita, M.Yamashita and H. Shigekawa, *Appl. Phys. Lett.* 85, 3268-3270 (2004).
3. O.Takeuchi M. Aoyama H. Kondo, Y. Terada and H.Shigekawa, *Jpn. J. Appl. Phys.* (2006) in press.
4. O.Takeuchi M. Aoyama and H.Shigekawa, *Jpn. J. Appl. Phys*. 44, 7B, 5354-5357 (2005).
5. O. Takeuchi and H. Shigekawa, "*Mono-cycle Photonics and Optical Scanning Tunneling Microscopy*" ed. M. Yamashita, H. Shigekawa, R. Morita, Springer Series in Optical Sciences, vol. 99 (2005).
6. H. Shigekawa, O. Takeuchi and M. Aoyama, *Science and Technology of Advanced Materials* 6, 582 (2005).
7. O. Takeuchi, S. Yoshida and H. Shigekawa, *Appl. Phys. Lett*. 84, 3645-3647 (2004).
8. S. Yoshida, J. Kikuchi, Y. Kanitani, O. Takeuchi, H. Oigawa and H. Shigekawa, *e-J. Surf. Sci. & Nanotechnol*, in press.
9. S. Yoshida, T. Kimura, O. Takeuchi, K. Hata, H. Oigawa, T. Nagamura, and H. Shigekawa, *Phys. Rev. B* 70, 235411 (2004).
10. S. Yasuda, T. Nakamura, M. Matsumoto and H. Shigekawa, *J. Am. Chem. Soc*. 125, 16430-16433 (2003).
11. H. Shigekawa, K. Miyake, M. Ishida, K. Hata, H. Oigawa, Y. Nannichi, R. Yoshizaki, A. Kawazu, T. Abe, T. Ozawa, T. Nagamura, *Jpn. J. Appl. Phys*. 35 L108-1084 (1996).
12. H. Shigekawa, K. Hata, K. Miyake, M. Ishida and S. Ozawa, *Phys. Rev. B* 55, 15448 (1997).
13. H. Shigekawa, K. Miyake, M. Ishida and K. Hata, *Jpn. J. Appl. Phys.* 36, L294-297 (1997).
14. S. Yoshida, T. Kimura, O. Takeuchi, K. Hata, H. Oigawa, T. Nagamura, H. Sakama, and H. Shigekawa, *Phys. Rev. B* 70, 235411 (2004).
15. K. Hata, S. Yoshida and H. Shigekawa, *Phys. Rev. Lett.* 89, 286104 (2002).
16. T. Kimura, S. Yoshida, O. Takeuchi, E. Matsuyama, H. Oigawa and H. Shigekawa, *Jpn. J. Appl. Phys.* 43, 7B, L990-L992 (2004).
17. K. Hata, Y. Sainoo and H. Shigekawa, *Phys. Rev. Lett*. 86, 3084-3087 (2001).
18. J. Shah, "*Ultrafast Spectroscopy of Semiconductors and Semiconductor Nanostructures"* Springer, Solid State Science Series (1999).
19. S. Weiss, D. Botkin, D. F. Ogletree, M. Salmeron, D. S. Chemla, *Phys. Stat. Sol.* (b) 188, 343-359 (1995).
20. M. R. Freeman, A. Y. Elezzabi, G. M. Steeves, and G. Nunes, Jr., *Surf. Sci.* 386, 290-300 (1997).
21. R. H. M. Greoeneveld and H. van Kempman, *Appl. Phys. Lett.* 69, 2294-2296 (1996).

22. N. N. Khusnatdinov, T. J. Nagle, and G. Nunes, Jr., *Appl. Phys. Lett*. 77, 4434-4436 (2000).
23. R. J. Hamers and D. G. Cahill, *J. Vac. Sci. Technol*. B9, 514-518 (1991).
24. S. Grafstroem, *J. Appl. Phys*. 91, 1717 (2002).
25. W. Pfeiffer, F. Sattler, S. Vogler, G. Gerber, J. Grand and R. Moller, *Appl. Phys. B: Lasers Opt.* 64, 265 (1997).